Effect of Boric Acid Content on the Structural and Optical Properties of MnS Films Prepared by Spray Pyrolysis Technique

M. Bedir[a,*], M. Öztaş[b], S.S. Çelik[a] and T. Özdemir[a]

[a]University of Gaziantep, Department of Engineering Physics, Gaziantep, Turkey

[b]University of Yalova, Chemical and Process Engineering, Yalova, Turkey

(Received May 13, 2013; revised version February 14, 2014; in final form April 14, 2014)

Boron doped MnS films were obtained by the spray pyrolysis method using the boric acid (H_3BO_3) as dopant source at a substrate temperature of 350 °C. The spray pyrolysis method has a wide range of application areas with a low cost well-suited for the manufacture of solar cells. The properties of boron doped MnS films were investigated as a function of doping concentration. The X-ray analysis showed that the films were polycrystalline fitting well with a hexagonal structure and have preferred orientation in the [002] direction. The optical band gap of the undoped and boron doped MnS films were found to vary from 3.38 to 3.20 eV. The changes observed in the energy band gap and structural properties of the films related to the boric acid concentration are discussed in detail.

DOI: 10.12693/APhysPolA.126.840

PACS: 81.15.Rs; 78.28.–e; 61.72.Vv; 61.05.cp; 68.55.Jk

1. Introduction

There has been a significant increase in the research work on the polycrystalline semiconductor materials due to their potential applications in various electronic and optoelectronic devices. The technological interest in polycrystalline based devices is mainly due to their very low production costs. Considerable attention has been paid to doped semiconductors as they offer multifunctional properties beyond those of ideal semiconductors [1].

In general, the characteristics of the films and related applications were dominated by the several factors, such as grain boundary, grain size, crystallinity, resistivity and optical properties, which are interrelated with utilized deposition and treatment methods and their variables [2, 3]. In particular, materials known as diluted magnetic semiconductors (DMS) have an interesting combination of magnetism and semiconductivity, so they have attracted widespread scientific attention due to their prospective applications in magneto-optical and spintronic devices. In DMS, the band electrons and holes strongly interact with the localized magnetic moments and cause a variety of interesting phenomena [4]. Manganese sulfide (MnS) VIIB–VIA is a wide gap DMS material (E_g = 3.1 eV) that is of potential interest in short wavelength optoelectronic applications such as in solar selective coatings, solar cells, sensors, photoconductors, optical mass memories [5–9].

In the recent years, extensive attention has been paid to the preparation and characterization of semiconductor sulfides as a consequence of their interesting properties and potential applications. MnS films can be prepared by different techniques such as radio-frequency sputtering [10], solvo-thermal synthesis [11], hydrothermal method [12], molecular beam epitaxy [13], thermal vacuum evaporation [14], successive ionic layer adsorption and reaction (SILAR) [15], chemical bath deposition (CBD) [16], and spray pyrolysis [17, 18]. *B*-doped ZnO (ZnO:B) thin film exhibits a promising characteristic of an effective technique for improving the conversion efficiency of Cu(In,Ga)Se_2 (CIGS) thin film solar cells [19], especially silicon thin film solar cells [20].

On the other hand, there exists some uncertain factors to influence the physical properties of ZnO:B thin film. Because of the smaller ion radius of boron, it can act as either interstitial boron or substitute boron in ZnO lattice [21]. The effects of boron doping on the properties of CdS thin films are investigated to evaluate proper doping level for good quality films by Lee [22].

The spray pyrolysis method used in this work is based on a chemical deposition technique where ionic solutions of the desired film materials are sprayed onto a preheated substrate. Films prepared by the spray pyrolysis technique are predominantly polycrystalline and their properties are significantly influenced by deposition procedures [23]. According to our knowledge, no report exists in the literature on the synthesis of boron doped MnS films by the spray pyrolysis technique. Therefore, we have tuned our attention to study the feasibility of the spray pyrolysis technique for the synthesis of boron doped MnS films. In this paper, the influence of boric acid concentration on the structural and optical properties of the sprayed boron doped MnS films are reported.

2. Experimental studies

The preparation of undoped and boron doped MnS films developed by the spray pyrolysis method has already been described [24]. In this technique, the boron

*corresponding author; e-mail: bedir@gantep.edu.tr

doped MnS films were deposited on heated glass substrates ($10 \times 10 \times 1.2$ mm^3) by spraying an aqueous solution in air atmosphere. The spray solutions are comprised of manganese chloride (0.7 M, Merck, $\geq$ 99%) and thiourea ($SC(NH_2)_2$) (0.7 M, Merck, $\geq$ 99%) in the deionized water. Deionized water was used as a solvent. Boron doped MnS films were deposited by adding boric acid (H_3BO_3) as a dopant source to the solution. The atomic percentage of dopants in (B/Mn) solution were 1.0 (boron doped MnS-1), 1.5 (boron doped MnS-2), and 3.0 (boron doped MnS-3) at.%. All films were deposited at the constant substrate temperature (T_s = 350 °C) which was measured by using electronically controlled a chromel–alumel thermocouple situated under the substrate. Before deposition, the glass substrates were ultrasonically cleaned in acetone solution, and then rinsed in de-ionized water. In this procedure, compressed air was used to atomize the solution containing the precursor compounds through a spray nozzle over the heated substrate; air is compressed from the atmosphere. Then the spraying solution is sprayed onto the glass substrate which is kept at the required temperature.

When the solution droplets reach the substrate surface, the following chemical reaction occurs:

$$MnCl_2 + SC(NH_2)_2 + 2H_2O \rightarrow MnS + 2NH_4Cl + CO_2$$

and by adding boric acid (H_3BO_3):

$$MnCl_2 + SC(NH_2)_2 + H_3BO_3 + 2H_2O \rightarrow MnS{:}B + 2NH_4Cl + CO_2 + 3OH.$$

The films were characterized by using a Pan–Alytical (X'Pert PRO) model X-ray diffractometer (XRD) with Cu K_α radiation (with 40 kV, 30 mA, $\lambda = 0.15406$ nm) at a scanning rate of 2 min^{-1} in the 2θ range from 10° to 70°. The scanning electro-microscopy (SEM) micrographs of all thin films were taken from JEOL JSM 6390 LV model scanning electromicroscopy. Perkin Elmer Lambda-2S Model UV–VIS–NIR spectrophotometer was used to determine the optical absorbance of the films as a function of wavelength at room temperature. A correction for substrate absorption was made by placing an identical uncoated glass substrate in the reference beam. The optical band gap energy E_g was determined by extrapolating the high absorption region of the curve to the energy axis [25].

3. Results and discussion

3.1. Structural studies

Figure 1 shows the XRD patterns of boron doped MnS films with different boric acid concentrations deposited at substrate temperature 350 °C. Films were characterized with the (100), (002) and (101) preferential planes. The preferential orientation of all films is found to be along (002) crystal plane (crystallites are oriented with the [002] direction perpendicular to the substrate, with a slight shift of the maximum towards higher 2θ values). This indicates that the boron doped MnS films prepared by the spray pyrolysis method are polycrystalline with the hexagonal structure and show a good c-axis orientation perpendicular to the substrate [18]. The intensity of (002) peak is increased with increasing B concentration up to 1.0 at.% and then the intensity of (002) peak is decreased.

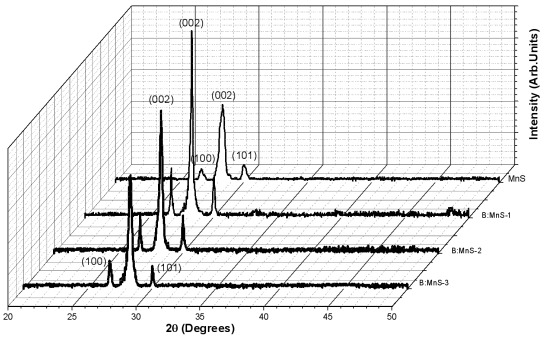

Fig. 1. XRD patterns of undoped and boron doped MnS films.

This behaviour can be understood by two competing processes; the increase in boron doping improves the stoichiometry of the films and the crystal quality. This indicates that boron ions are substituted at manganese ions sites up to 1.0 at.% after that B–B intragrain cluster is evaluated.

XRD pattern of highly boron doped (1.5 and 3.0 at.%) MnS is shown in Fig. 1 and the inset shows the B–B cluster intragrain. It is observed that the XRD intensity depends strongly on the boric acid concentrations. The maximum of the XRD intensity is illustrated by the pronounced peak at a boric acid concentration of 1.0 at.%. Thus, increasing the dopant level results in a change in preferred growth (002) direction. The spray deposition of 1.0 at.% boron doped MnS deposited at a substrate temperature of 350 °C is found to be optimum for the deposition of good quality boron doped MnS films at the specified spray conditions. It is shown that there is a critical doping value in the starting solution for which the characteristics of the boron doped MnS films has a minimum value, corresponding to the maximum crystal grain size value measured for these films. Consequently, the characteristics of boron doped MnS films prepared by the spray pyrolysis process depend strongly on the boron incorporation at the films. A similar behavior has already been observed by Pawar et al. [26].

It is also shown in Fig. 1 that the initial increase in the XRD peaks can be explained by the creation of new nucleating centers due to the B dopant atoms. The subsequent decrease in the XRD peaks for the high doping level could be explained by two factors; firstly, by the saturation of the newer nucleating centers and secondly, due to the change in the energy absorption at the time of collision, and of the physical and chemical interaction between adatoms and the film. For boron doped films, the grain size initially increases with an increase in dopant contents (up to 1.0%). Then, there is a decrease

in the crystal grain size with the increase in the boric acid concentrations, which may be due to the sufficient increase in the supply of thermal energy for recrystallization. This trend suggests that boron dopant creates newer nucleation centers, which in turn, would change the nucleation type from homogeneous to heterogeneous, and deteriorate the crystalline structure at high doping level.

The grain size of MnS and the boron doped MnS films were estimated for the (002) plane by using the Scherrer formula [27]:

$$d = \frac{\lambda}{D\cos\theta}, \tag{1}$$

where d is the grain size, λ is the X-ray wavelength, D is the angular line width of the half maximum intensity and θ is the Bragg angle. Table shows the various grain parameters of the undoped and boron doped MnS films which are associated to the (002) peak.

TABLE

Various grain parameters of the undoped and boron doped MnS films.

Substrate temperature T_s [°C]		2θ [degrees]	(hkl)	Lattice constant [nm]	Grain size [nm]	Microstrain ε [$\times 10^{-3}$]	Dislocation density ρ [$\times 10^{13}$] [line m^{-2}]	Band gap energy E_g [eV]
350	MnS	28.30	(002)	6.3021	30.5539	12.6052	57.9608	3.38
	boron doped MnS-1	28.41	(002)	6.2716	38.9619	9.2089	57.6990	3.20
	boron doped MnS-2	28.39	(002)	6.2802	36.9572	10.4215	57.7740	3.23
	boron doped MnS-2	28.34	(002)	6.2933	33.1032	11.6342	57.8862	3.29

From these results, we can see that the fundamental effect of the boron is related to an increase in the size of the crystallites, and a decrease in the lattice parameter, the band gap energy, the dislocation density and the microstrain. As the boric acid concentration increases, the intensity of MnS (002) peak increases and this peak becomes narrower indicating an improvement in the crystallinity. This means that the grain size of the films increase with increasing up to the boric acid content 1.0% (see Table). The XRD intensity depends strongly on the boric acid concentration permitted for maximum XRD intensity, which is illustrated by the pronounced peak with dopant contents (up to 1.0%). It shows that MnS films maintain the (002) preferred growth up to 1.0% boric acid contents. It is also observed that the addition of boric acid contents increases the full width at half maximum (FWHM) due to the destruction of the crystal structure and reduction in the grain size. It may be possible that this drastic change in grain size is due to the large difference in ionic radius of manganese and boron.

The decrease in the grain size is correlated with the broadening of the XRD peak. Smaller crystallite size results in a higher density of grain boundaries, which behaves as barriers for carrier transport and traps for free carrier. Hence, a decrease in the crystallite size can cause an increase in the grain boundary scattering [28]. This observations correlates with the results of XRD patterns.

The microstrain (ε) developed in the sprayed undoped and boron doped MnS films was calculated from the equation [29],

$$\varepsilon = \frac{D\cos\theta}{4}, \tag{2}$$

where D is the full width at half maximum of the (100), (002) and (101) peaks. It is observed from Table that the microstrain (ε) exhibits a slow decreasing trend with increasing boric acid concentration up to 1.0%. This type of change in microstrain may be due to the predominant recrystallization process in the polycrystalline films and due to the movement of interstitial Mn atoms from inside the crystallites to its grain boundary which dissipate and lead to a reduction in the concentration of lattice imperfections [30, 31]. This is due to the crystallinity of the films being improved which can be correlated with the increase in the grain size and the XRD results.

The dislocation density ρ is determined by the relation [32]:

$$\rho = \frac{15\varepsilon}{aD}. \tag{3}$$

The variation in the dislocation density with boric acid concentration is shown in Table. The dislocation density (ρ) is defined as the length of dislocation lines per unit of the crystal, and the small ρ means that the crystallization of the films is good. As seen from Table, dislocation density (ρ) exhibits a decreasing trend up to 1.0% boric acid contents and then increases with higher doping levels. Also, it is shown that the microstrain and the dislocation density decrease with an increase in grain size, which indicates a lower number of lattice imperfec-

tions. This may be due to a decrease in the occurrence of grain boundaries because of an increase in the grain size of the film with increase in boric acid concentration up to 1.0%. These parameters indicate the formation of high quality boron doped MnS films deposited on the well cleaned glass substrate by the spray pyrolysis method with dopant contents (up to 1.0%).

This observation correlates that the grain size increases but the dislocation density and the microstrain decreases at the lower doping level. Since the dislocation density and the microstrain are the manifestation of dislocation network in the films, the decrease in the microstrain and the dislocation density indicates the formation of higher quality films at lower doping level [33].

3.2. Optical studies

Undoped and boron doped MnS films are a direct transition semiconductor and its absorption coefficient (α) and optical band gap energy (E_g) are interrelated [34]. The band gap energy of the films was calculated from Eq. (4). The $(\alpha h\nu)^2$ versus $h\nu$ (energy) is plotted. The bandgap energy values of MnS films with the atomic percentage of dopants in (B/Mn) solution with (a) 0.0%, (b) 1.0%, (c) 1.5%, (d) 3.0% are given in Fig. 2.

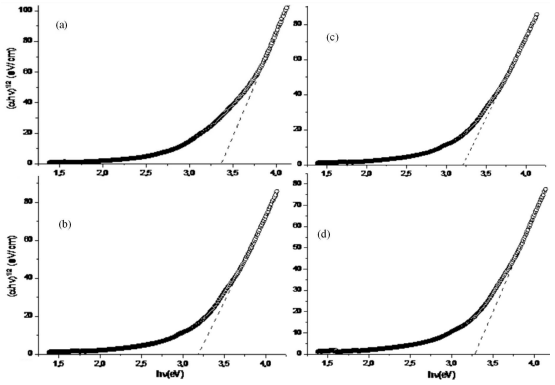

Fig. 2. Bandgap energy values of MnS films with the atomic percentage of dopants in (B/Mn) solution with (a) 0.0%, (b) 1.0%, (c) 1.5%, (d) 3.0%.

The plots are parabolic in nature and the number of inflexions reveal the number of transitions. At inflexion, the tangential extrapolation to x-axis (energy) gives the band gap energy

$$\alpha = \frac{A}{h\nu}(h\nu - E_g)^{\frac{1}{2}}, \tag{4}$$

where $h\nu$ is the photon energy, E_g denotes the optical energy bandgap, and A is the characteristic parameter (independent of photon energy) for respective transitions. It is seen from Table that the decrease in the optical band gap of the films with an increase in dopant contents (up to 1.0%) can be attributed to the increase in the grain size.

Another reason could be the improving crystallinity with increasing grain size and this may be due to the extension of electronic states of the impurity phase, precipitates and clusters, into the band gap of MnS. It is seen at higher doping levels that the band gap was increased, and the grain size of boron doped MnS films were decreased. The change in E_g with the atomic percentage of dopants in (B/Mn) solution and grain size was observed in boron doped MnS films. Therefore, the band gap energy shift of boron doped MnS films in our study can be attributed to the quantum size effect. The change in E_g with atomic percentage of dopants in (B/Mn) solution can be understood by the quantum size effect observed in the films of semiconductors. From the results of Table, E_{opt} for the MnS films with the B doping concentration 1.0, 1.5, and 3.0 at.%, is 3.20, 3.23, and 3.29 eV, respectively. This broadening in the band gap is known as the Moss–Burstein shift [35]. According to the Moss–Burstein theory, in heavily doped manganese sulphide films, the donor electrons occupy states at the bottom of the conduction band. Since the Pauli principle prevents states from being doubly occupied and optical transitions are vertical, the valence electrons require extra energy to be excited to higher energy states in the conduction band. Therefore, the optical band gap (E_{opt}) of doped manganese sulphide is broader than that of undoped zinc oxide films. It may be also another reason that defects are accumulated at the grain boundaries. Smaller grain size results in a tensile strain arising from thermal mismatch between the MnS film and the substrate. This indicates that the presence of large number of grain boundaries increases the defects in the film. The change in E_g with boric acid contents can be correlated with the change of the structural properties of the films.

3.3. SEM studies

The morphologies of MnS films prepared from solution containing 0, 1.0, 1.5, and 3.0 at.% boric acid contents as dopant are shown in Fig. 3. SEM gives valuable information regarding the shape and size of the grains on the surface of the deposited films. Figure 3 shows the SEM

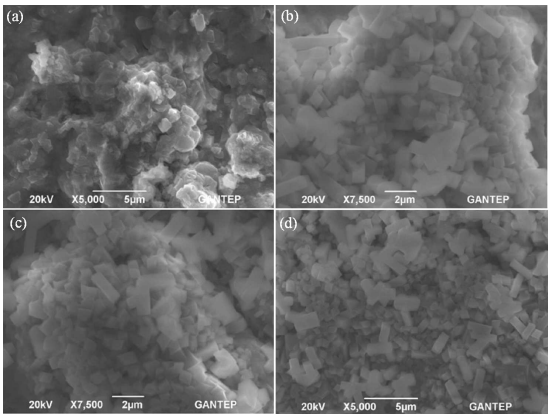

Fig. 3. SEM micrographs of the undoped and boron doped MnS films at different molar ratios: (a) 0.0%, (b) 1.0%, (c) 1.5%, (d) 3.0%.

image of MnS films prepared at 350° substrate temperature, and reveals rectangular shape grains, which are aggregated. The observed change in the morphology indicates that the boron atoms act as nucleation centers in the vacancy sites of MnS. The result of the analysis indicates that the boron atoms can influence the grain size. It may be also that the roughness of MnS films directly decrease with increasing the boric acid content (1.0 at.%). Such decreased roughness could be explained as a consequence of a reduction in the grain size with a uniform and more compact surface morphology as evidenced from the SEM images. The SEM images show that the surface morphology of the films is strongly dependent on the concentration of boric acid. This observation correlates with the change in the grain size.

4. Conclusion

The study of the structural and optical properties of undoped and boron doped MnS films obtained by the spray pyrolysis technique shows that they are strongly dependent on the boric acid concentration. The obtained results confirmed that the nature of the MnS films leads to significant changes in the structural and optical properties of these films. From the structural and optical analyses, it is observed that B incorporation plays a significant role in the crystalline and structural properties of the MnS films. Using the optical investigations including the band gap, it was determined that the band gap of MnS:B films decreases with increase of the boric acid concentrations up to 1.0%, due to the improved crystallization of the films and the changes in grain size. Therefore, it can be said that 1.0% boric acid incorporations are the most suitable boric acid contents, to improve the crystallinity of MnS films.

References

[1] J. Poortmans, V. Arkhipov, *Thin Film Solar Cells Fabrication, Characterization and Applications*, Wiley, New York 2006.

[2] M. Ortega-Lopez, A. Morales-Acevedo, *Thin Solid Films* **330**, 96 (1998).

[3] J.M. Peza-Tapia, V.M. Sanchez-Resendiz, M. Albor-Aguilera, J.J. Cayente-Romero, L.R. De Leon-Gutierrez, M. Ortega-Lopez, *Thin Solid Films* **490**, 142 (2005).

[4] N. Badera, B. Godbole, S.B. Srivastava, P.N. Vishwakarma, Sharath, L.S. Chandra, J. Deepti, V.G. Sathe, V. Ganesan, *Sol. Energy Mater Sol. Cells* **92**, 1646 (2008).

[5] D. Fan, X. Yang, H. Wang, Y. Zhang, H. Yan, *Physica B* **337**, 165 (2003).

[6] B. Piriou, J.D. Ghys, S. Mochizuki, *J. Phys., Condens. Matter* **6**, 7317 (1994).

[7] R. Tappero, P. D' Arco, A. Lichanot, *Chem. Phys. Lett.* **273**, 83 (1997).

[8] C.D. Lokhande, A. Ennaoui, P.S. Patil, M. Giersig, M. Muller, K. Diesner, H. Tributsch, *Thin Solid Films* **330**, 70 (1998).

[9] D. Hobbs, J. Hafner, *J. Phys., Condens. Matter* **11**, 8197 (1999).

[10] S.A. Mayen-Hernandez, S.J. Sandoval, R.C. Perez, G.T. Delgado, B.S. Chao, O.J. Sandoval, *J. Cryst. Growth* **256**, 12 (2003).

[11] J. Mu, Z.F. Gu, L. Wang, Z.Q. Zhang, H. Sun, S.Z. Kang, *J. Nanopart. Res.* **10**, 197 (2008).

[12] Z. Pingtang, Z. Qiumei, H. Xianliang, T. Hao, H. Kaixun, *J. Cryst. Growth* **310**, 4268 (2008).

[13] L. David, C. Bradford, X. Tang, T.C.M. Graham, K.A. Prior, B.C. Cavenett, *J. Cryst. Growth* **251**, 591 (2003).

[14] D. Sreekantha Reddy, D. Raja Reddy, N. Koteeswara Reddy, K.R. Gunasekhar, R.P. Vijayalakshmi, B.K. Reddy, P. Sreedhara Reddy, *Solid State Commun.* **142**, 466 (2007).

[15] H.M. Pathan, S.S. Kale, C.D. Lokhande, S.H. Han, O.S. Joo, *Mater. Res. Bull.* **42**, 1565 (2007).

[16] D. Fan, H. Wang, Y.C. Zhang, J. Cheng, B. Wang, H. Yan, *Mater. Chem. Phys.* **80**, 44 (2003).

[17] M.R.I. Chowdhury, J. Podder, A.B.M.O. Islam, *Cryst. Res. Techn.* **46**, 267 (2011).

[18] A. Yilmaz, *Phys. Scr.* **83**, 045603 (2011).

[19] Y. Hagiwara, T. Nakada, A. Kunioka, *Sol. Energy Mater. Sol. Cells* **67**, 267 (2001).

[20] J. Hupkes, B. Rech, S. Calnan, O. Kluth, U. Zastrow, H. Siekmann, M. Wuttig, *Thin Solid Films* **502**, 286 (2006).

[21] B.N. Pawar, S.R. Jadkar, M.G. Takwale, *J. Phys. Chem. Solids* **66**, 1779 (2005).

[22] J. Lee, *Thin Solid Films* **170**, 451 (2004).

[23] M. Bedir, M. Öztas, D. Korkmaz, Y. Özdemir, *Arab. J. Sci. Eng.* **39**, 503 (2014).

[24] M. Oztas, M. Bedir, O.F. Bakkaloglu, R. Ormanci, *Acta Phys. Pol. A* **107**, 525 (2005).

[25] V.M. Gopalrao, *J. Electr. Eng.* **2**, 54 (2014).

[26] B.N. Pawar, S.R. Jadkar, M.G. Takwal, *J. Phys. Chem. Solids* **66**, 1779 (2005).

[27] B.D. Cullity, *Elements of X-ray Diffraction*, Addison–Wesley, Boston 1978, p. 99.

[28] H. Kim, J.S. Horwitz, G. Kushto, A. Pique, Z.H. Kafafi, C.M. Gilmore, D.B. Chrisey, *J. Appl. Phys.* **88**, 6021 (2000).

[29] C.K. De, N.K. Mishra, *Indian J. Phys. A* **71**, 530 (1997).

[30] F.A. Kroger, *The Chemistry of Imperfect Crystals*, North-Holland, Amsterdam 1964.

[31] C.F. Rong, G.D. Watkins, *Phys. Rev. Lett.* **58**, 1486 (1987).

[32] M. Bedir, M. Oztas, O.F. Bakkaloglu, R. Ormanci, *Eur. Phys. J. B* **45**, 465 (2005).

[33] N. Jabena Begum, K. Ravichandrann, *J. Phys. Chem. Solids* **74**, 841 (2013).

[34] G. Kim, J. Bang, Y. Kim, S.K. Rout, S.I. Woo, *Appl. Phys. A* **97**, 821 (2009).

[35] B.E. Sernelius, K.F. Berggren, Z.C. Jim, I. Hamberg, C.G. Granqvist, *Phys. Rev. B* **37**, 10244 (1988).